

# IDENTIFIED-PARTICLE PRODUCTION AND SPECTRA WITH THE ALICE DETECTOR IN $pp$ AND Pb–Pb COLLISIONS AT THE LHC\*

ROBERTO PREGHENELLA

for the ALICE Collaboration

Centro Studi e Ricerche e Museo Storico della Fisica “Enrico Fermi”, Rome, Italy  
and

Dipartimento di Fisica dell’Università and Sezione INFN, Bologna, Italy  
`preghenella@bo.infn.it`

*(Received December 12, 2011)*

Thanks to its unique capabilities the ALICE experiment can measure the production of identified particles and resonances over a wide momentum range both in  $pp$  and Pb–Pb collisions at the LHC. In this report, particle-identification detectors and techniques, as well as achieved performance, are shortly reviewed. The current results on hadron transverse momentum spectra measured in  $pp$  collisions at  $\sqrt{s} = 0.9$  TeV and 7 TeV, and in Pb–Pb collisions at  $\sqrt{s_{NN}} = 2.76$  TeV are shown. In particular, proton–proton results on particle production yields, spectral shapes and particle ratios are presented as a function of the collision energy and compared to previous experiments and commonly-used Monte Carlo models. Particle spectra, yields and ratios in Pb–Pb are measured as a function of the collision centrality and the results are compared with published RHIC data in Au–Au collisions at  $\sqrt{s_{NN}} = 0.2$  TeV and predictions for the LHC.

DOI:10.5506/APhysPolB.43.555

PACS numbers: 25.75.Ag, 25.75.Dw

## 1. Introduction

ALICE (A Large Ion Collider Experiment) is a general-purpose heavy-ion experiment at the CERN LHC (Large Hadron Collider) aimed at studying the physics of strongly-interacting matter and the quark-gluon plasma. A unique design has been adopted for the ALICE detector to fulfil tracking and particle-identification requirements [1]. Thanks to these features,

---

\* Presented at the Conference “Strangeness in Quark Matter 2011”, Kraków, Poland, September 18–24, 2011.

the experiment is able to identify hadrons in a wide momentum range by combining different detecting systems and techniques, as discussed in Section 2. Results on hadron spectra and yields at mid-rapidity are presented in Section 3 for  $pp$  collisions at  $\sqrt{s} = 0.9$  TeV and 7 TeV, and in Section 4 for Pb–Pb collisions at  $\sqrt{s_{NN}} = 2.76$  TeV.

## 2. Particle identification

In this section, the particle-identification (PID) detectors relevant for the analyses presented in this paper are briefly discussed, namely the *Inner Tracking System* (ITS), the *Time-Projection Chamber* (TPC) and the *Time-of-Flight* detector (TOF). A detailed review of the ALICE experiment and of its PID capabilities can be found in [1]. The ITS is a six-layer silicon detector located at radii between 4 and 43 cm. Four of the six layers provide  $dE/dx$  measurements and are used for particle identification in the non-relativistic ( $1/\beta^2$ ) region. Moreover, using the ITS as a standalone tracker enables one to reconstruct and identify low-momentum particles (below 200 MeV/ $c$ ) not reaching the main tracking systems. The TPC is the main central-barrel tracking detector of ALICE and provides three-dimensional hit information and specific energy-loss measurements with up to 159 samples. With the measured particle momentum and  $\langle dE/dx \rangle$  the particle type can be determined by comparing the measurements against the Bethe–Bloch expectation. The TOF detector is a large-area array of Multigap Resistive Plate Chambers (MRPC) and covers the central pseudorapidity region ( $|\eta| < 0.9$ , full azimuth). Particle identification is performed by matching momentum and trajectory-length measurements performed by the tracking system with the time-of-flight information provided by the TOF system. The total time-of-flight resolution is about 85 ps in Pb–Pb collisions (about 120 ps in  $pp$  collisions) and it is determined by the time resolution of the detector itself and by the start-time resolution.

The transverse momentum spectra of primary  $\pi^\pm$ ,  $K^\pm$ ,  $p$  and  $\bar{p}$  are measured at mid-rapidity ( $|y| < 0.5$ ) combining the techniques and detectors described above. Primary particles are defined as prompt particles produced in the collision and all decay products, except products from weak decay of strange particles. The contribution from the feed-down of weakly-decaying particles to  $\pi^\pm$ ,  $p$  and  $\bar{p}$  and from protons from material are subtracted by fitting the data using Monte Carlo templates of the DCA<sup>1</sup> distributions. Particles can also be identified in ALICE via their characteristics decay topology or invariant mass fits. This, combined with the direct identification of the decay daughters, allows one to reconstruct weakly-decaying particles and hadronic resonances with an improved signal-to-background ratio.

---

<sup>1</sup> Distance of Closest Approach to the reconstructed primary vertex.

### 3. Results in $pp$ collisions

The transverse momentum spectra of primary  $\pi^\pm$ ,  $K^\pm$ ,  $p$  and  $\bar{p}$  have been measured in minimum-bias  $pp$  collisions at  $\sqrt{s} = 0.9$  TeV and 7 TeV. The measurements performed at  $\sqrt{s} = 0.9$  TeV and the details of the analysis are already published in [2]. The results of the analysis performed at  $\sqrt{s} = 7$  TeV were reported at this conference [3]. The ratios  $K/\pi$  and  $p/\pi$  as a function of  $p_T$  are shown in figure 1 comparing measurements at  $\sqrt{s} = 0.9$  TeV and 7 TeV. Both ratios do not show evident energy dependence and the same holds for the  $p_T$ -integrated production ratios which are also observed to be rather independent of the collision energy from 0.9 TeV to 7 TeV. Moreover, no difference between  $p/\pi^+$  and  $\bar{p}/\pi^-$  ratios is observed leading to a constant value of about 0.05 and vanishing baryon/antibaryon asymmetry at LHC as already reported in [4]. The comparison with Monte Carlo generators shows that the  $p_T$ -dependent  $K/\pi$  ratio is underestimated at high  $p_T$  by recent PYTHIA tunes. The same holds for the  $p/\pi$  ratio, though a better agreement with the data is observed for PYTHIA D6T.

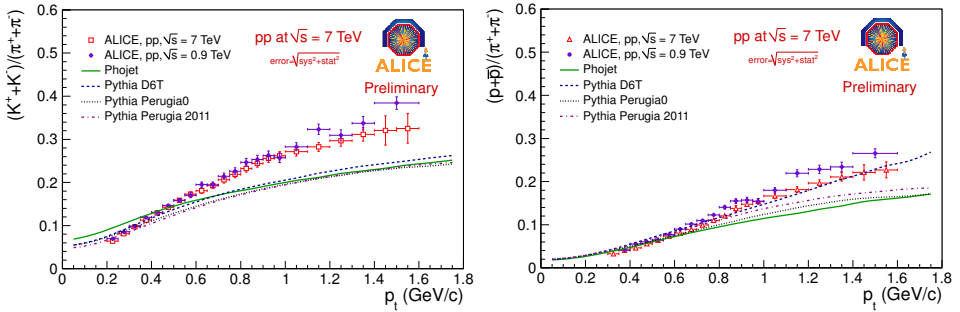


Fig. 1.  $K/\pi$  (left) and  $p/\pi$  (right) production ratios as a function of  $p_T$  measured in  $pp$  collisions at  $\sqrt{s} = 0.9$  TeV and 7 TeV compared to various Monte Carlo models at  $\sqrt{s} = 7$  TeV.

Measurements of the production of multi-strange baryons  $\Xi \rightarrow \Lambda + \pi \rightarrow p + \pi + \pi$  and  $\Omega \rightarrow \Lambda + K \rightarrow p + \pi + K$  and of hadronic resonances  $K^* \rightarrow K + \pi$  and  $\phi \rightarrow K^+ + K^-$  in  $pp$  collisions were also reported at this conference (see [5, 6], respectively). When compared to Monte Carlo event generators, multi-strange baryon production is underpredicted by various PYTHIA tunes, though the most recent Perugia-2011 tune shows an overall better agreement with the data, in particular in the high  $p_T$  region.  $\phi$  resonance production is rather well described by PHOJET, whereas in PYTHIA Perugia-2011 it is slightly under-predicted at low  $p_T$ . It is worth to stress here that an overall good agreement between the data and PYTHIA Perugia-2011 tune is observed for charged-kaons but not for resonance production,

as can be deduced from figure 2. On the other hand, there is still some work for tuning model for resonances (especially baryons) and multi-strange baryon production.

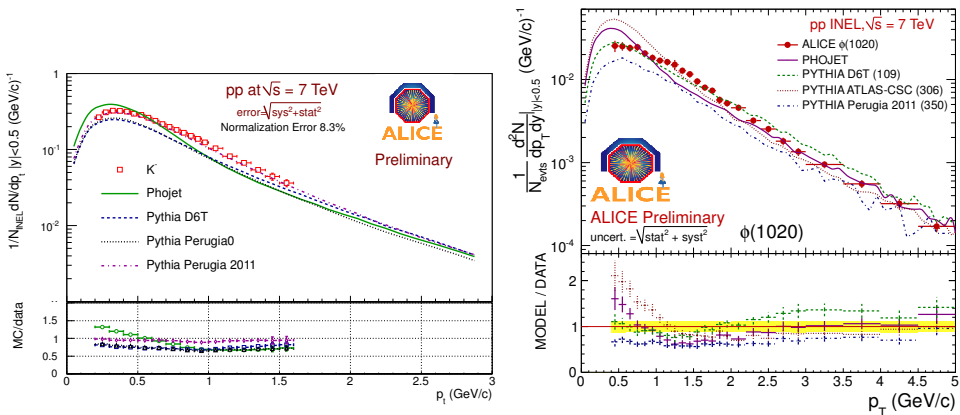


Fig. 2. Transverse momentum spectra of  $K^-$  (left) and  $\phi$  (right) in  $pp$  collisions at  $\sqrt{s} = 7$  TeV compared to various Monte Carlo models.

#### 4. Results in Pb–Pb collisions

Hadron  $p_T$  spectra have been measured in several centrality classes (see [7] for details on centrality selection) from 100 MeV/c up to 3 GeV/c for pions, from 200 MeV/c up to 2 GeV/c for kaons and from 300 MeV/c up to 3 GeV/c for protons and antiprotons. Individual fits to the data are performed using a blast-wave parametrization [8] to extrapolate the spectra outside the measured  $p_T$  range. The measured spectra and corresponding fits are shown in figure 3 for primary  $\pi^-$  (top),  $K^-$  (middle) and  $\bar{p}$  (bottom). Average transverse momenta  $\langle p_T \rangle$  and integrated production yields  $dN/dy$  are obtained using the measured data points and the extrapolation.

As reported in [3], the spectra are observed to be harder than at RHIC for similar  $dN_{ch}/d\eta$ . A detailed study of the spectral shapes has been done in order to give a quantitative estimate of the thermal freeze-out temperature  $T_{fo}$  and the average transverse flow  $\langle \beta \rangle$ . A combined blast-wave fit of the spectra has been performed in the  $p_T$  ranges 0.3–1.0 GeV/c, 0.2–1.5 GeV/c and 0.3–3.0 GeV/c for pions, kaons and protons, respectively. While the  $T_{fo}$  parameter is sensitive to the pion fit range because of feed-down of resonances<sup>2</sup> the transverse flow  $\langle \beta \rangle$  measurement is not, being dominated by the proton spectral shape. The results obtained on the thermal freeze-out

<sup>2</sup> This effect will be investigated in details in the future.

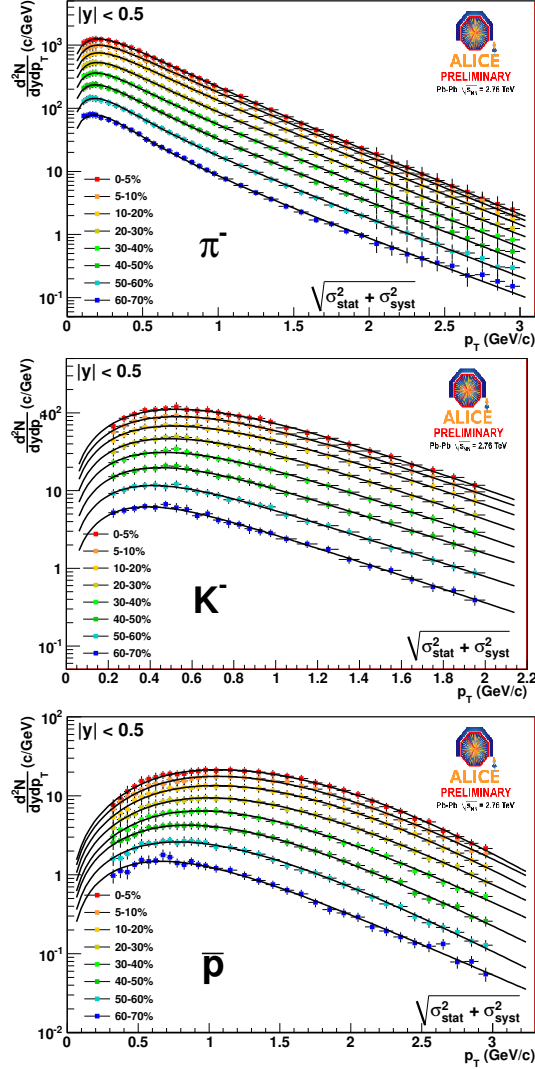


Fig. 3. Transverse momentum spectra of primary  $\pi^-$  (top),  $K^-$  (middle),  $\bar{p}$  (bottom) and corresponding fits in Pb-Pb collisions at  $\sqrt{s_{NN}} = 2.76$  TeV.

properties in different centrality bins are compared with similar measurements performed by the STAR Collaboration at lower energies in figure 4 (left). A stronger radial flow is observed with respect to RHIC, being about 10% larger in the most central collisions at the LHC. The data are also compared to predictions from hydrodynamic models. As already reported in [11] the pure hydrodynamic prediction [12] cannot reproduce the proton shape.

A similar disagreement was observed when comparing proton elliptic flow  $v_2$  to the same model [13]. A new calculation has been performed using a hybrid model which adds a hadronic rescattering and freeze-out stage to the viscous dynamics [14]. These new predictions [15] are compared to the data in figure 4 (right) and the agreement with the proton shape is better than in a pure hydrodynamic picture. This suggests that extra flow builds up in the hadronic phase. The difference in the proton yield can be ascribed to the fact that the model derives yields from a thermal model with  $T_{\text{ch}} = 165$  MeV. It is worth to mention that this model also reproduces the shape of elliptic flow of identified particles as reported at this conference [16].

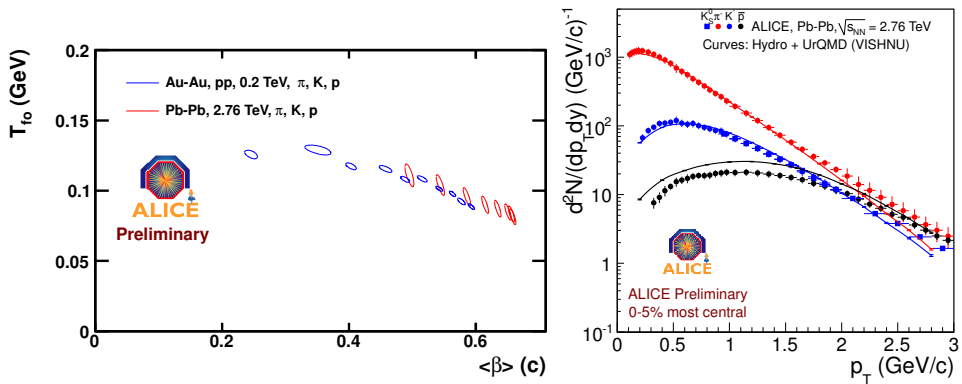


Fig. 4. Thermal freeze-out parameters  $T_{\text{fo}}$  and  $\langle\beta\rangle$  from combined blast-wave fits compared to RHIC data (left).  $\pi^-$ ,  $K^-$ ,  $\bar{p}$  spectra in 0–5% central Pb–Pb collisions compared to hydrodynamic model predictions [14, 15] (right).

Antiparticle/particle integrated production ratios are observed to be consistent with unity for all particle species in all centralities suggesting that the baryo-chemical potential  $\mu_B$  is close to zero as expected at LHC energies. Figure 5 (left) compares ALICE results with RHIC data in Au–Au collisions at  $\sqrt{s_{NN}} = 0.2$  TeV [9] for the 0–5% most central collisions. The  $p_T$ -integrated  $K^-/\pi^-$  and  $\bar{p}/\pi^-$  ratios and the production of multi-strange baryons in Pb–Pb collisions were also reported at this conference (see [17] and [18], respectively). The  $K^-/\pi^-$  production nicely follows the trend measured at RHIC. The  $\bar{p}/\pi^-$  production ratio ( $\sim 0.05$ ) is significantly lower than the value expected from statistical model predictions ( $\sim 0.07$ – $0.09$ ) with a chemical freeze-out temperature of  $T_{\text{ch}} = 160$ – $170$  MeV at the LHC [10]. The measured yields of several particles normalized to the pion yield in 0–5% central collisions are compared to thermal model predictions in figure 5 (right). With a temperature of  $T_{\text{ch}} = 164$  MeV predicted by Andronic *et al.* [10] the model reproduces both kaon and multi-strange baryon production but

overestimates the protons. The same model can be tuned to reproduce proton yields with an *ad hoc*  $T_{\text{ch}} = 148 \text{ MeV}$ , though multi-strange baryon production is underestimated in this case.

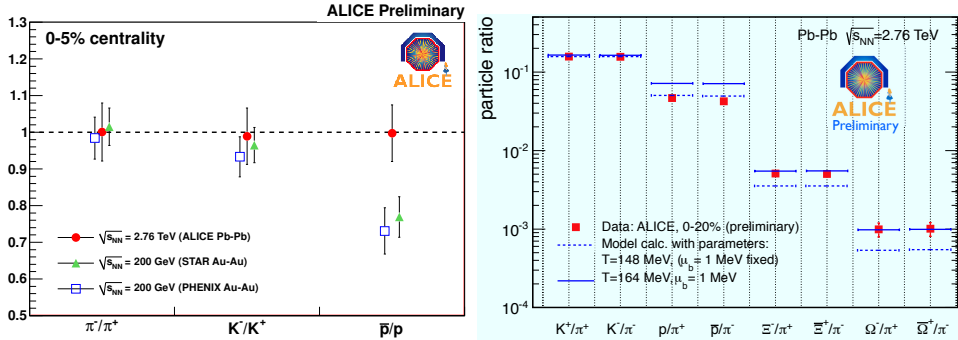


Fig. 5. Antiparticle/particle production ratios in the 0–5% most central Pb–Pb collisions [9] (left). Hadron-production ratios compared to thermal model predictions [10] (right).

## 5. Conclusions

The transverse momentum spectra of  $\pi^\pm$ ,  $K^\pm$ ,  $p$  and  $\bar{p}$  have been measured with ALICE in  $pp$  collisions at  $\sqrt{s} = 0.9 \text{ TeV}$  and  $7 \text{ TeV}$  and in Pb–Pb collisions at  $\sqrt{s_{NN}} = 2.76 \text{ TeV}$ , demonstrating the excellent PID capabilities of the experiment. Proton–proton results show no evident  $\sqrt{s}$  dependence in hadron production ratios. Monte Carlo generators do not reproduce hadron ratios and multi-strange baryon production yet, though a good agreement between the data and PYTHIA Perugia-2011 is observed for charged kaons. In Pb–Pb collisions the  $\bar{p}/\pi^-$  integrated ratio is significantly lower than statistical model predictions with a chemical freeze-out temperature  $T_{\text{ch}} = 160\text{--}170 \text{ MeV}$ . The average transverse momenta and the spectral shapes indicate a  $\sim 10\%$  stronger radial flow than at RHIC energies. The comparison with recent hydrodynamic calculations suggests that extra flow builds up in the hadronic phase.

## REFERENCES

- [1] ALICE Collaboration, *J. Phys. G* **32**, 1295 (2006); *J. Instrum.* **3**, S08002 (2008).
- [2] ALICE Collaboration, *Eur. Phys. J.* **C71**, 1655 (2011).
- [3] B. Guerzoni [ALICE Collaboration], *Acta Phys. Pol. B Proc. Suppl.* **5**, 271 (2012).

- [4] ALICE Collaboration, *Phys. Rev. Lett.* **105**, 072002 (2010).
- [5] A. Maire [ALICE Collaboration], *Acta Phys. Pol. B Proc. Suppl.* **5**, 231 (2012).
- [6] D. Gangadharan [ALICE Collaboration], *Acta Phys. Pol. B Proc. Suppl.* **5**, 277 (2012).
- [7] ALICE Collaboration, *Phys. Rev. Lett.* **106**, 032301 (2011).
- [8] E. Schnedermann, J. Sollfrank, U. Heinz, *Phys. Rev.* **C48**, 2462 (1993).
- [9] STAR Collaboration, *Phys. Rev.* **C79**, 034909 (2009); PHENIX Collaboration, *Phys. Rev.* **C69**, 034909 (2004); BRAHMS Collaboration, *Phys. Rev.* **C72**, 014908 (2005).
- [10] J. Cleymans *et al.*, *Phys. Rev.* **C74**, 034903 (2006); A. Andronic *et al.*, *Phys. Lett.* **B673**, 142 (2009).
- [11] M. Floris [ALICE Collaboration], [arXiv:1108.3257v1 \[hep-ex\]](#).
- [12] C. Shen, U. Heinz, P. Huovinen, H. Song, [arXiv:1105.3226v2 \[nucl-th\]](#).
- [13] R. Snellings [ALICE Collaboration], Quark Matter 2011, Annecy, France, May 23–28, 2011.
- [14] U. Heinz, C. Shen, H. Song, [arXiv:1108.5323v1 \[nucl-th\]](#).
- [15] U. Heinz, H. Song, private communication.
- [16] F. Noferini [ALICE Collaboration], *Acta Phys. Pol. B Proc. Suppl.* **5**, 329 (2012).
- [17] A. Kalweit [ALICE Collaboration], *Acta Phys. Pol. B Proc. Suppl.* **5**, 225 (2012).
- [18] M. Nicassio [ALICE Collaboration], *Acta Phys. Pol. B Proc. Suppl.* **5**, 237 (2012).